

Extended Coherence Time with Atom-Number Squeezed Sources

Wei Li, Ari K. Tuchman, Hui-Chun Chien, and Mark A. Kasevich
Physics Department, Stanford University, Stanford, CA 94305
(Dated: October 2, 2018)

Coherence properties of Bose-Einstein condensates offer the potential for improved interferometric phase contrast. However, decoherence effects due to the mean-field interaction shorten the coherence time, thus limiting potential sensitivity. In this work, we demonstrate increased coherence times with number squeezed states in an optical lattice using the decay of Bloch oscillations to probe the coherence time. We extend coherence times by a factor of 2 over those expected with coherent state BEC interferometry. We observe quantitative agreement with theory both for the degree of initial number squeezing as well as for prolonged coherence times.

Experimental requirements for precision atom interferometry are well suited to many of the coherence properties of Bose-Einstein condensates [1, 2, 3, 4, 5]. BECs possess narrower momentum distributions than those of ultra-cold atomic gases, which removes the need for velocity selection during initial state preparation. The longer coherence length of a condensate improves phase contrast, and colder temperatures reduce ensemble expansion during long interferometer interrogation times. Furthermore, for confined atom-interferometers [6, 7, 8] which require spatial separation of a wavepacket in close proximity to a guiding surface, the superfluid properties of a BEC offer an additional advantage. The mean-field interaction energy in BECs provides an energy gap to external excitations, effectively decoupling the atomic proof-mass from the physical sensor.

On the other hand, the coherence time for BEC interferometry can be significantly reduced with respect to cold atom sources. Prior to separation, two linked condensates have relative number fluctuations which support a well defined relative phase. However, when separated, the interplay of a large on-site mean-field interaction with large number variance causes rapid dephasing [9]. This concern has been addressed previously by using either dilute condensates [10] or alternatively, Fermi gases which do not suffer from density broadening mechanisms [11]. It is possible, however, to retain some of the benefits of BEC interferometry while minimizing mean-field induced decoherence. The generation of atom-number squeezed states from a BEC in an optical lattice [12, 13] has offered the possibility to create states with reduced sensitivity to mean-field decay mechanisms.

In this work, we study the characteristic time scale for which an array of BECs preserves relative phase information after becoming fragmented, and we observe prolonged coherence times for number squeezed states. The coherence time is probed through the decay time of a Bloch oscillation, and we find quantitative agreement with theoretical predictions.

The theoretical treatment for a BEC in an optical lattice begins with the Bose-Hubbard Hamiltonian [14].

$$H = -\gamma \sum_i (\hat{a}_{i+1}^\dagger \hat{a}_i + H.c.) + \sum_i \varepsilon_i \hat{N}_i + \frac{g\beta}{2} \sum_i \hat{a}_i^\dagger \hat{a}_i^\dagger \hat{a}_i \hat{a}_i \quad (1)$$

where $g\beta$ represents the mean-field interaction energy and γ is the inter-well tunneling matrix element with both terms dependent on lattice depth. ε_i denotes the external potential term and \hat{a}_i and \hat{a}_i^\dagger represent single particle annihilation and creation operators respectively at the i th lattice site. N_i denotes local atom number which is replaced by the central well occupation N in the discussion below.

In the regime of low lattice potential and correspondingly large tunneling ($N\gamma \gg g\beta$) the many-body ground state of the system is described by a superfluid state with local atom number uncertainty $\sigma(N) = \sqrt{N}$. As the potential barrier is adiabatically raised, the interplay of the interaction and tunneling terms renders number fluctuations energetically unfavorable. In the Bogoliubov limit, number fluctuations decrease with increasing lattice potential as $\sigma_S(N) = \left(\frac{N^2}{1+Ng\beta/2\gamma}\right)^{\frac{1}{4}}$ [15], with commensurately increasing on-site phase fluctuations. In the limit of $N\gamma \ll g\beta$, the system enters the Mott-Insulating regime, where the wavefunction at each site approximates an atom-number Fock state [13].

We fragment this array by frustrating tunneling between adjacent lattice sites. In previous work, this has been achieved by diabatically raising a large potential barrier [12, 16]. In this work, we frustrate tunneling by applying a large energy gradient across the array. This method is preferred since the on-site mean field energy (the third term on the right of Eq. 1) is unaffected by this process. This sudden localization is analogous to a beam splitter which instantly separates an ensemble into two distinct paths. The many-body ground state does not have time to react to the perturbation, and therefore an array of independent, localized many-atom states is formed. The initial array state is no longer in the ground state, and therefore, the array phase collapses.

Relative phase dispersion between adjacent wells is intuitively understood by considering an array initially prepared in a shallow lattice potential. After fragmentation,

each coherent state $|\alpha\rangle$ can be expanded as a superposition of atom-number Fock states, $|\alpha\rangle = \sum_n \frac{\alpha^n e^{-\frac{1}{2}|\alpha|^2}}{\sqrt{n!}} |n\rangle$, where the phase of each term in the superposition evolves as $\Delta\phi_{n,i} = \mu(n, \varepsilon_i)t/\hbar$, and $\mu = ng\beta + \varepsilon_i$ is the local chemical potential. Each number term in the superposition evolves at a different rate, leading to relative phase dispersion with a characteristic decay time τ_c . The decay of array coherence is seen in the time dependence of the expectation value of the order parameter $|\langle \hat{a} \rangle| = \sqrt{N}e^{-N(g\beta)^2 t^2/2}$ where $\tau_c = (\sqrt{N}g\beta)^{-1}$ [9]. This coherence time can be prolonged, however, by reducing the number of terms in the initial atom-number state superposition. For squeezed states with reduced number uncertainty $\sigma_S(N)$, the coherence time increases as

$$\tau_s = (g\beta\sigma_S(N))^{-1} = (g\beta\left(\frac{N^2}{1 + Ng\beta/\gamma}\right)^{\frac{1}{4}})^{-1}. \quad (2)$$

We measure τ_c for different initial number variances by studying the decay of coherent Bloch oscillations [17, 18, 19]. An energy gradient $\varepsilon_i = Ei$ is applied to the array where E is written in units of energy. This drives an oscillatory response in the quasimomentum, q , of the atomic Bloch state with a period $T = \hbar/2\pi E$. Although Bloch oscillations are traditionally observed for conditions where the array is described by bands delocalized spatially over many lattice sites, they also occur for spatially localized wavefunctions described in the Wannier-Stark basis [20]. We isolate the lattice sites when $E \gg \gamma$ but ensure that E is not too large as to cause particle loss through Zener tunneling [2]. The Bloch oscillation is observed experimentally by interferometrically following the evolution of the relative phase between adjacent wells $\Delta\Phi = q\lambda/2\hbar$, where $\lambda/2$ is the lattice period. Dispersion in momentum space provides a quantitative indication of dephasing.

The apparatus used in this experiment has been described in detail [12]. We load 10^8 ^{87}Rb atoms into a time-orbiting potential (TOP) trap. Evaporative cooling generates a BEC in the $|F = 2, m_F = 2\rangle$ state with 1500 atoms, density $\rho \sim 10^{12} \text{ cm}^{-3}$ and temperature $\sim 0.2 T_c$. Atom number is determined with absorptive imaging with 20% shot-to-shot fluctuations and is consistent with the observed condensate fraction as a function of temperature.

We trap the condensate in a 1-D, vertically oriented optical lattice. The lattice light is red detuned from the ^{87}Rb resonance and has $1/e$ radii of $60 \mu\text{m}$. The potential depth, U , (measured in E_R , where $E_R = \hbar^2 k^2/2m$ and $k = 2\pi/\lambda$ with $\lambda = 852 \text{ nm}$) is calibrated using three independent methods which all agree to within 10%. We first measure U by driving an even parity parametric excitation from the lowest energy band [21]. We also measure the period of Kapitza-Dirac diffraction by suddenly turning on the optical lattice [22]. Finally, we measure the frequency of Josephson tunneling, which is valid for

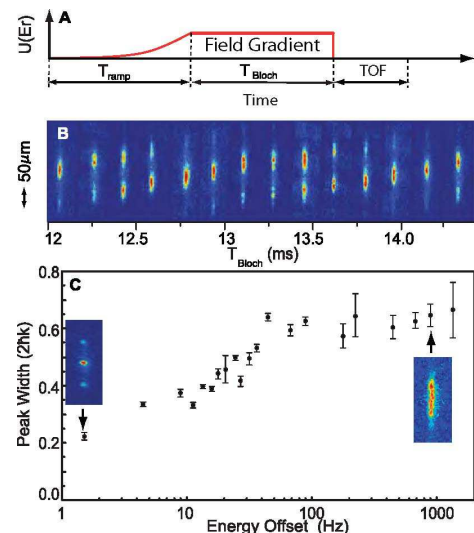


FIG. 1:

A) Lattice intensity is shown for the experimental sequence. The lattice intensity is ramped up in $T_{\text{ramp}} = 350$ ms and then held constant for T_{Bloch} during which time a magnetic field gradient is applied. The lattice and magnetic fields are turned off and the atoms ballistically expand for a 12 ms Time of Flight (TOF) before being imaged with a probe pulse. B) Absorptive images indicating a Bloch oscillation are shown. C) Peak width vs. energy offset E is shown with widths converted to units of $2\hbar k$. Insets show absorptive images both with and without dephasing

low lattice depths, $U < 12 E_R$ [23]. For lattice depths explored in this work ($5 < U < 24 E_R$) we calculate $2\pi \times 4 < \gamma/\hbar < 2\pi \times 250$ Hz, $2\pi \times 0.6 < g\beta/\hbar < 2\pi \times 1.8$ Hz and $103 < N < 150$, and the vertical $1/e$ condensate array radius ranges between 7 – 10 lattice sites.

After state preparation in the optical lattice (Fig. 1A), we drive a Bloch oscillation by applying a magnetic field gradient along the array axis. We probe the coherence of the Bloch oscillation by releasing the array, rapidly switching off the lattice within 500 ns. The interferometric signal is absorptively imaged with single atom detection sensitivity. Fig. 1B shows images depicting a Bloch oscillation with $T = 1.1$ ms, taken with $U = 10 E_R$ and $E/\hbar = 2\pi \times 900$ Hz.

We ensure that adjacent sites are decoupled during T_{Bloch} by varying E and measuring the width of the central interference peak. An increased width indicates dephasing of the Bloch oscillation. We apply the field gradient for 40 ms before releasing the array. We see in Fig. 1C that for small E the Bloch oscillation shows minimal dephasing. However, for large energy offsets the peak width increases, saturating at our resolution limit for $\gamma \sim E$, where $\gamma/\hbar = 2\pi \times 39$ Hz for $U = 12 E_R$.

We next quantify the degree of number squeezing generated at a given lattice depth. We adiabatically increase the lattice intensity and then interfere the array, generating an interference pattern with sharp peaks on top of a

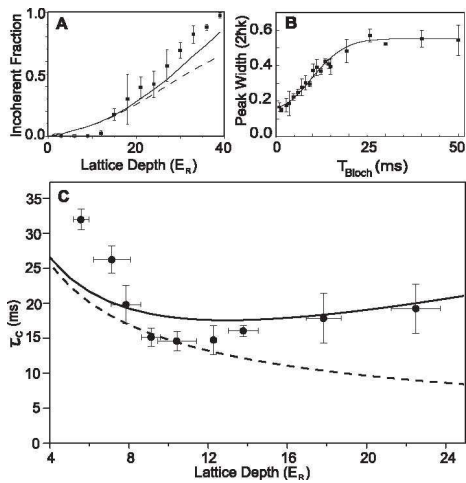


FIG. 2:

A) The fraction of atoms observed in the incoherent background of the interference signature is plotted vs. lattice depth. This fraction from the simulated interference of an array of Gaussian wavepackets is shown with a solid line. The calculated quantum depletion vs. lattice depth is shown with a dashed line. B) Peak width is plotted vs. T_{Bloch} for $U = 10 E_R$ and $E/\hbar = 2\pi \times 900$ Hz. Solid line is a fit to data to extract $\tau_c = 14.2 \pm 1.3$ ms. C) τ_c is plotted vs. lattice depth. Solid (dashed) line denotes theoretical dephasing of number squeezed (coherent) states.

broad incoherent background. We extract this incoherent fraction by fitting the signal to a function with three narrow Gaussian peaks and a fourth broad peak. For very low lattice depths the incoherent background is within our noise floor. The observed incoherent fraction shown in Fig. 2A is a quantitative metric of number squeezing as seen by comparison with two theoretical models. First we simulate the interference pattern from an array of Gaussian BEC wavefunctions with $\sigma_S(N)$ determined by our experimental conditions [12, 15]. We extract the simulated incoherent background (shown with a solid line) by using the same fit function as used with our experimental data. Second, we calculate the degree of quantum depletion [15], the fraction of atoms not characterized by an order parameter, expected at a given lattice depth. We equate this depletion fraction with the incoherent fraction of an interference signal, shown with a dashed line. Note that our observed quantum depletion is significantly higher than that observed in Ref. [24] due to our densities which are nearly two orders of magnitude lower.

With demonstrated control over number squeezing and site localization, we explore the dependence of τ_c on initial number variance. Using the experimental sequence in Fig. 1A, we take an absorptive image of the interfering atoms for different lattice depths with E kept constant. We fit the central vertical peak to a Gaussian to determine the width as a function of T_{Bloch} . We measure τ_c by fitting the data as in Fig. 2B to

$w(t) = w_f - (w_f - w_0)e^{-(t/\tau_c)^2}$ [9]. w_f is the maximum observed width representing a fully dephased signature, and w_0 is the peak width prior to any phase dispersion.

Fig. 2C shows the summary graph plotting τ_c vs. lattice depth, where increased lattice depth reflects increased number squeezing. The theoretical τ_c for isolated coherent states and number squeezed states (Eq. 2) are shown with dashed and solid lines respectively. For very low lattice depths τ_c is longer than expected for either coherent state or squeezed state dephasing. This is likely due to insufficient isolation between wells when γ is large. However, we cannot significantly increase E at this lattice depth without introducing Zener tunneling losses. For intermediate lattice depths with near-Poissonian number variance, we observe good correlation of τ_c with that expected for isolated coherent state condensates.

For deeper lattice depths, however, we measure long coherence times which are in quantitative agreement with theoretical number squeezed state dephasing. For number squeezed states prepared at $U = 22.5 E_R$, $\tau_c = 19.3 \pm 3.5$ ms. This represents an increase of a factor of 2.1 over the expected decay time of an array of coherent states in the same lattice potential. It is interesting to note that here squeezing extends the coherence time; typically, the enhanced fragility of squeezed states to loss mechanisms results in reduced coherence times [25].

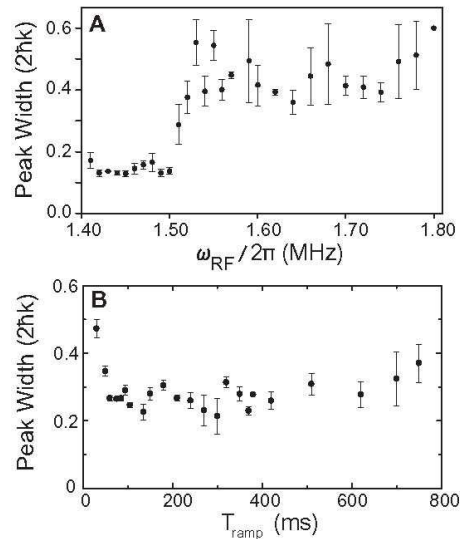


FIG. 3:

A) Peak width vs. $\omega_{\text{RF}}/2\pi$. $T_c = 1.6$ MHz for a BEC in the bare harmonic trap. B) Peak width vs. T_{ramp}

To eliminate other potential sources of dephasing, we investigate the effects of finite temperature and the adiabaticity of our lattice ramp on the interferometric peak width observed in Bloch oscillations. We prepare condensates at different temperatures by varying the final frequency ω_{RF} of the evaporative cooling stage. As seen

in Fig. 3A, we observe no change in peak width for $2\pi \times 1.40 < \omega_{\text{RF}} < 2\pi \times 1.50$ MHz with $U = 16 E_R$. However, at $\omega_{\text{RF}} = 2\pi \times 1.51$ MHz we observe a sudden onset of phase broadening. To avoid this thermal dephasing regime all data was taken with $\omega_{\text{RF}} = 2\pi \times 1.44$ MHz. Note that this critical temperature in the lattice is different from the BEC transition temperature in a bare harmonic trap (corresponding to $\omega_{\text{RF}} = 2\pi \times 1.6$ MHz).

In Fig. 3B, we investigate the dependence of peak width on lattice intensity ramp speed. A balance is required to avoid losses due to lattice heating with very long ramp times and non-adiabaticity effects with short ramp times. We find that peak width is insensitive to ramp speed for $80 < T_{\text{ramp}} < 620$ ms.

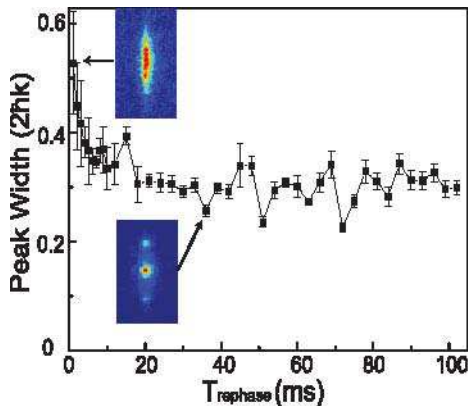


FIG. 4: Peak width is plotted vs. continued hold time in lattice after removing the external field gradient, T_{rephase} . Insets are absorptive images showing initial dephasing of the phase contrast and subsequent revival.

As a final consideration, we explore the possibility for coherence restoration after complete dephasing. We use the same experimental sequence as in Fig. 1A, with $U = 10 E_R$ and $T_{\text{Bloch}} = 80$ ms, ensuring that dephasing has occurred. This time, however, after turning off the magnetic field gradient we continue to hold the atoms in the optical potential before interfering them. We see phase contrast return nearly completely after a rephasing time $\tau_r \sim 10$ ms as shown in Fig. 4. While the details of this rephasing mechanism require further investigation, a two-well model predicts this time to be determined by the generalized Josephson frequency $\omega_J = \sqrt{Ng\beta\gamma}$. Our observed rephasing time is in excellent agreement with this prediction for our parameters [26].

In conclusion, we have demonstrated that number squeezed states in an optical lattice can extend coherence times for interferometry. We have obtained quantitative

agreement with theory both in calibrating the number variance of our initial state as well as in observed coherence times with number squeezed states. For sensitivity considerations in practical interferometers, however, note that extended coherence times come with the price of increased phase noise due to number squeezing. Future work will explore this tradeoff in optimizing absolute sensor performance.

We acknowledge funding support from DARPA and the MURI on Quantum Metrology sponsored by ONR. The work of A.K.T. was supported by an IC fellowship, sponsored by NGA.

-
- [1] M. Andrews, *et al.*, *Science* **275**, 637 (1997).
 - [2] B. Anderson and M. Kasevich, *Science* **282**, 39 (1998).
 - [3] Y. Torii, *et al.*, *Phys. Rev. A* **61**, 041602 (2000).
 - [4] S. Gupta, K. Dieckmann, Z. Hadzibabic, D. Pritchard, *Phys. Rev. Lett.* **89**, 140401 (2002).
 - [5] Y. Shin, *et al.*, *Phys. Rev. Lett.* **92**, 050405 (2004).
 - [6] Y. Wang, *et al.*, *Phys. Rev. Lett.* **94**, 090405 (2005).
 - [7] S. Gupta, K. Murch, K. Moore, T. Purdy, D. Stamper-Kurn, *Phys. Rev. Lett.* **95**, 143201 (2005).
 - [8] A. Günther, *et al.*, *Phys. Rev. Lett.* **95**, 170405 (2005).
 - [9] A. Imamoglu, M. Lewenstein and L. You, *Phys. Rev. Lett.* **78**, 2511 (1997).
 - [10] J. M. Reeves, *et al.*, *Phys. Rev. A* **72**, 051605R (2005).
 - [11] G. Roati, *et al.*, *Phys. Rev. Lett.* **92**, 230402 (2004).
 - [12] C. Orzel, A. K. Tuchman, M. L. Fenselau, M. Yasuda and M. A. Kasevich, *Science* **291**, 2386 (2001).
 - [13] M. Greiner, O. Mandel, T. Esslinger, T. Hansch and I. Bloch, *Nature* **415**, 39 (2002).
 - [14] D. Jaksch, C. Bruder, J. I. Cirac, C. W. Gardiner and P. Zoller, *Phys. Rev. Lett.* **81**, 3108 (1998).
 - [15] K. Burnett, M. Edwards, C. Clark and M. Shotton, *J. Phys. B* **35**, 1671 (2002).
 - [16] M. Greiner, O. Mandel, T. Esslinger, T. Hansch and I. Bloch, *Nature* **419**, 51 (2002).
 - [17] F. Bloch, *Z. Phys.* **52**, 555 (1928).
 - [18] M. Ben Dahan, E. Peik, J. Reichel, Y. Castin and C. Salomon, *Phys. Rev. Lett.* **76**, 4508 (1996).
 - [19] O. Morsch, *et al.*, *Phys. Rev. Lett.* **87**, 140402 (2001).
 - [20] S. Sachdev, K. Sengupta, S. Girvin, *Phys. Rev. B* **66**, 075128 (2002).
 - [21] C. Schori, T. Stoferle, H. Moritz, M. Kohl, and T. Esslinger, *Phys. Rev. Lett.* **93**, 240402 (2004).
 - [22] J. Denschlag, *et al.*, *J. Phys. B* **35**, 3095 (2002).
 - [23] F. S. Cataliotti, *et al.*, *Science* **293**, 843 (2001).
 - [24] K. Xu, *et al.*, *Phys. Rev. Lett.* **96**, 180405 (2006).
 - [25] J. Stockton, J.M. Geremia, A. Doherty, H. Mabuchi, *Phys. Rev. A* **67**, 022112 (2003).
 - [26] A. Smerzi, S. Fantoni, S. Giovanazzi, S.R. Shenoy, *Phys. Rev. Lett.* **79**, 4950 (1997).